Large Helical Device (LHD)

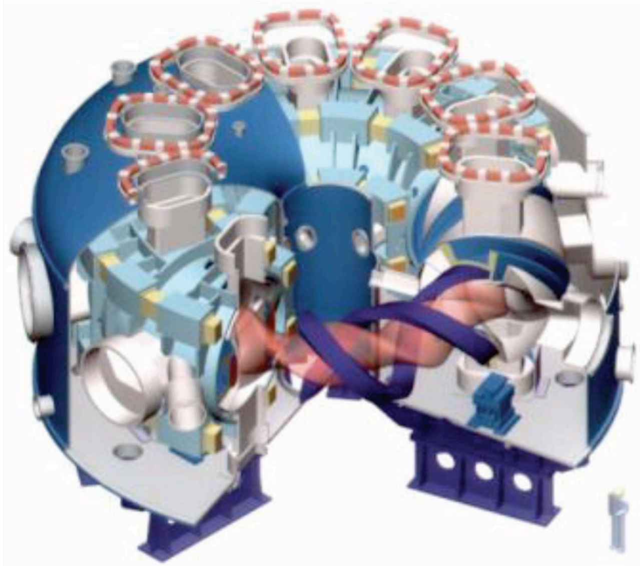

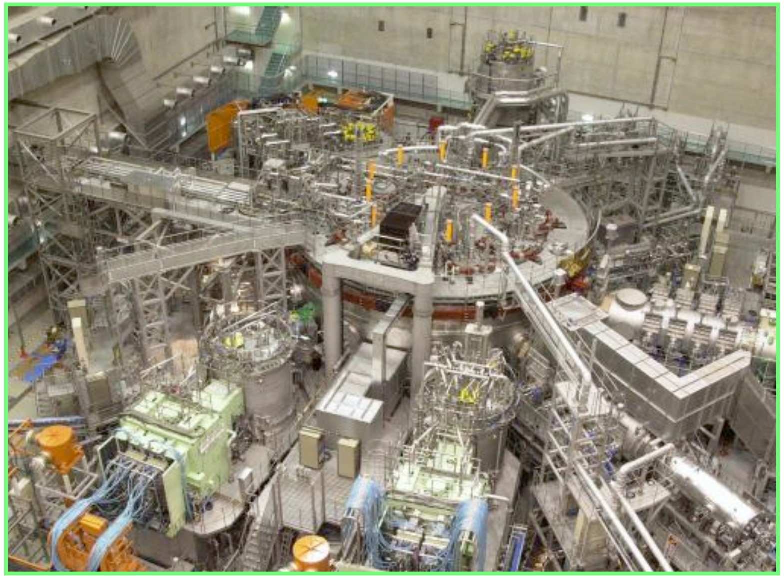

Heliotron configuration

No net plasma current required

➡ Suitable for steady-state operation

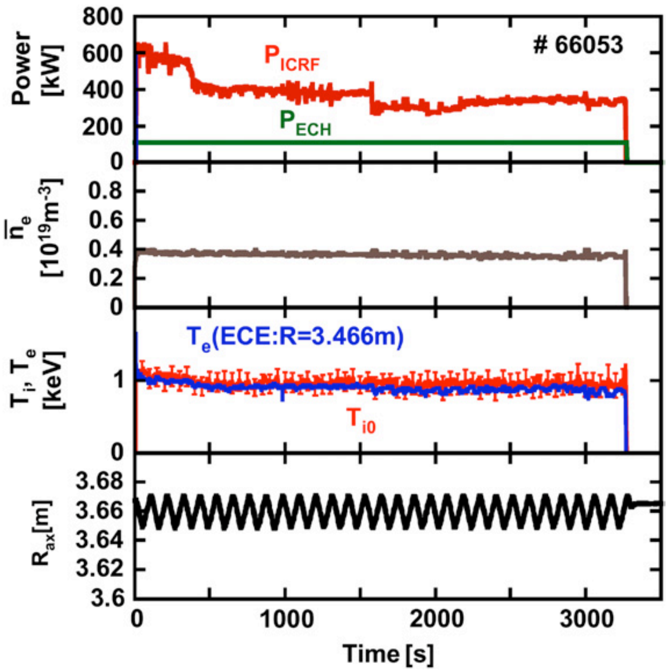

1-hour discharge

Max. parameters

$R = 3.9$ m	$n = 1.1 \times 10^{21}$ m^{-3}
$a = 0.6$ m	$T_e = 10$ keV
$V = 30$ m^3	$T_H = 6.9$ keV
$B = 3 \sim 4$ T	$\langle\beta\rangle = 5$ %

Classification of particle orbits

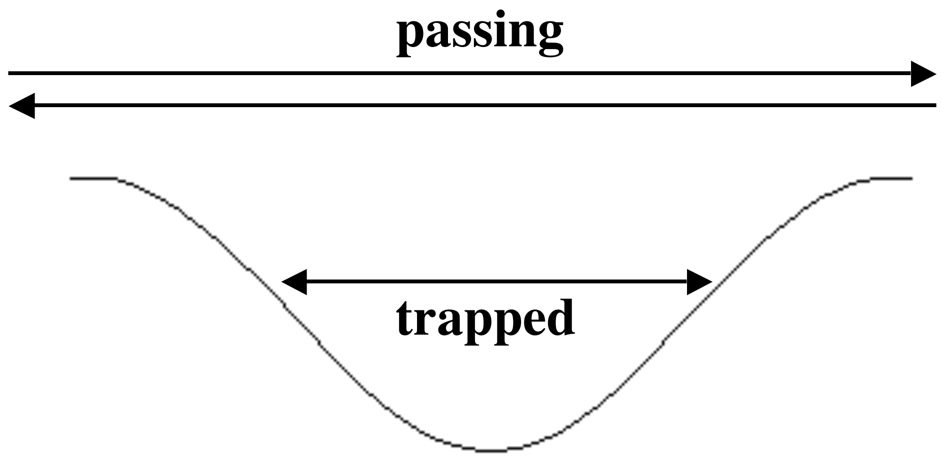

Tokamak

$B = B_0\ (1 - \varepsilon_t \cos\ \theta\ )$

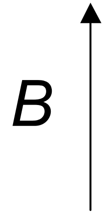

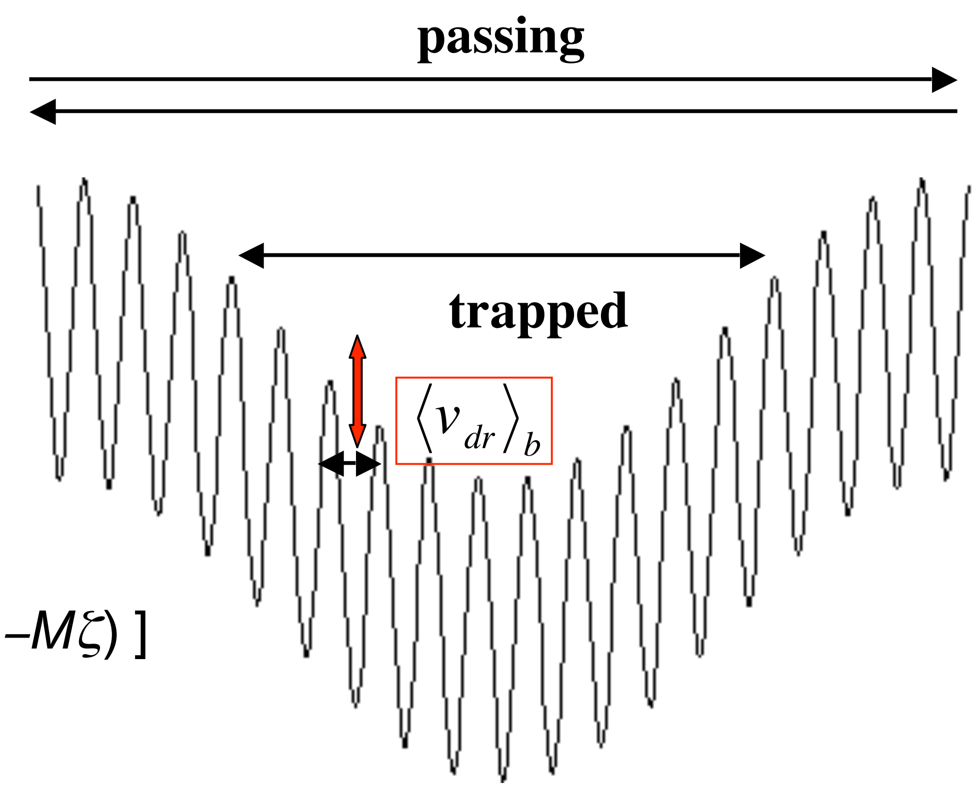

Helical System

$B = B_0\ [\ 1 - \varepsilon_t \cos\ \theta - \varepsilon_h \cos\ (L\theta - M\zeta)\ ]$

Collisionless Time Evolution of Zonal Flows in Helical Systems

[Sugama & Watanabe, PRL (2005), Phys.Plasmas (2006)]

$k\,\rho_i < 1$

Zonal-flow potential

$$\frac{e\phi_{\mathbf{k}_\perp}(t)}{T_i} = \mathcal{K}(t)\frac{e\phi_{\mathbf{k}_\perp}(0)}{T_i} + \frac{1}{n_0\langle k_\perp^2 a_i^2\rangle}\int_0^t dt'\ \mathcal{K}(t-t')\left\{1-\frac{2}{\pi}\left\langle(2\epsilon_H)^{1/2}\{1-g_{i1}(t-t',\theta)\}\right\rangle\right\}^{-1}$$
$$\times\left\langle\int_{\kappa^2<1} d^3v\ e^{-ik_r\overline{v}_{dri}(t-t')}\ F_{i0}S_{i\mathbf{k}_\perp}(t') + \int_{\kappa^2>1} d^3v\ F_{i0}S_{i\mathbf{k}_\perp}(t')\{1+ik_r(\Delta_r-\langle\Delta_r\rangle_{\rm po})\}\right\rangle$$

Response function = **GAM component** + **Residual component**

$$\mathcal{K}(t) = \mathcal{K}_{GAM}(t)[1-\mathcal{K}_L(t)] + \mathcal{K}_L(t)$$

$$\mathcal{K}(t\ =\ 0)\ =\ 1 \qquad \mathcal{K}(t)\ \rightarrow\ \mathcal{K}_L(t)\ \text{as}\ \mathcal{K}_{GAM}(t)\rightarrow 0$$

GAM response function $\qquad \mathcal{K}_{GAM}(t) = \cos(\omega_G t)\exp(\gamma t)$

Long-time response function $\qquad \boxed{\mathcal{K}_L(t) \equiv \frac{1-(2/\pi)\langle(2\epsilon_H)^{1/2}\{1-g_{i1}(t,\theta)\}\rangle}{1+G+\mathcal{E}(t)/\left(n_0\langle k_\perp^2 a_i^2\rangle\right)}}$

$$\boxed{\mathcal{E}(t) = \frac{2}{\pi}n_0\left[\langle(2\epsilon_H)^{1/2}\{1-g_{i1}(t,\theta)\}\rangle - \frac{3}{2}\langle k_\perp^2 a_i^2\rangle \times\langle(2\epsilon_H)^{1/2}\{1-g_{i2}(t,\theta)\}\rangle + \frac{T_i}{T_e}\langle(2\epsilon_H)^{1/2}\{1-g_{e1}(t,\theta)\}\rangle\right]}$$

$\mathcal{E}(t)$ represents effects of shielding of potential due to helical-ripple-trapped particles.

Comparison between Zonal-Flow Responses in Tokamak and Helical Plasmas

($q = 1.5$, $\varepsilon_t = 0.1$, $k_r a_i = 0.131$)

Helical ripples enhance GAM damping rate.

Tokamak

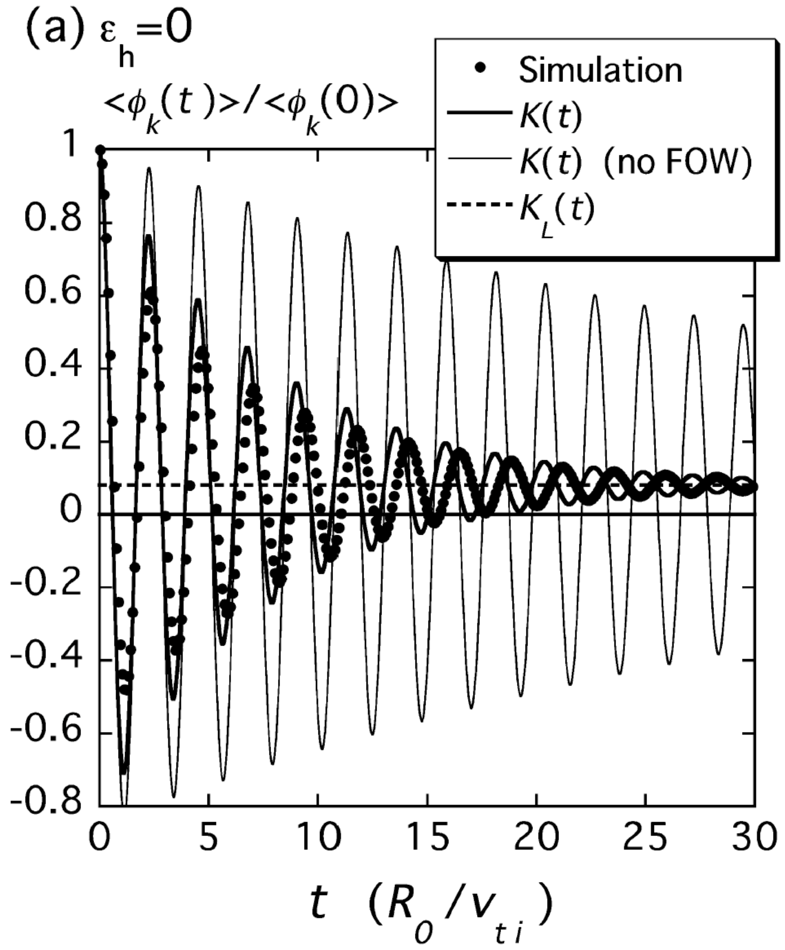

Helical plasma (*L*=2, *M*=10)

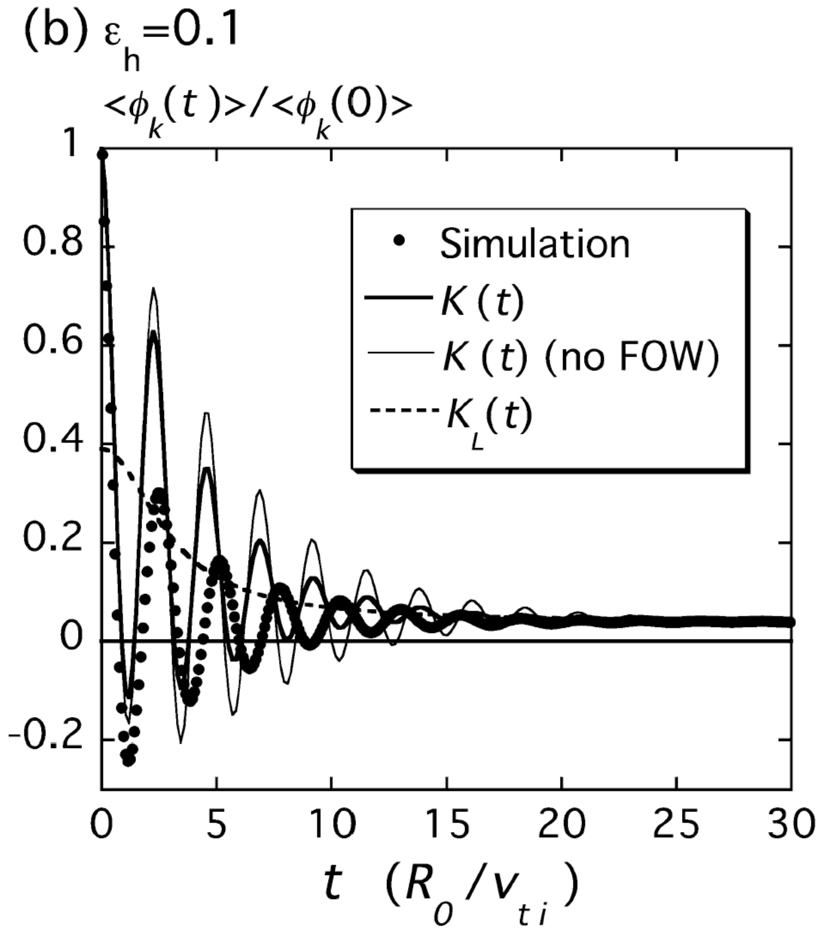

The long-time limit of the response kernel

$$\begin{aligned}\mathcal{K}_> &\equiv \lim_{t/\tau_c \to +\infty} \mathcal{K}_L(t) \\ &= \langle k_\perp^2 a_i^2 \rangle \left[1 - (2/\pi)\langle (2\epsilon_H)^{1/2} \rangle\right] \\ &\quad \times \left\{ \langle k_\perp^2 a_i^2 \rangle [1 - (3/\pi)\langle (2\epsilon_H)^{1/2} \rangle + G] \right. \\ &\qquad \left. + (2/\pi)(1 + T_i/T_e)\langle (2\epsilon_H)^{1/2} \rangle \right\}^{-1}\end{aligned}$$

depends on the depth of helical ripples ε_H as well as on the radial wave number k_r.

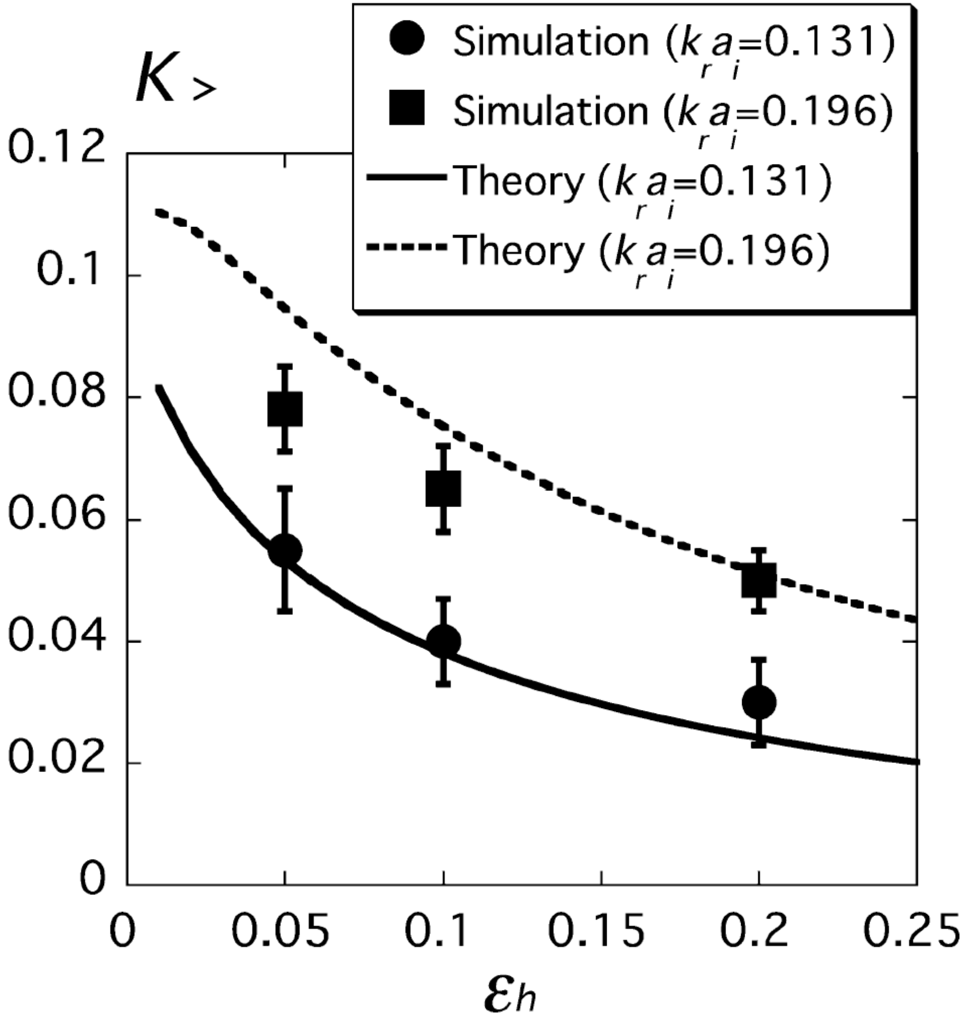

The perturbed ion gyrocenter distribution is given by the analytical solution:

$$\delta f_{i\mathbf{k}_\perp}^{(\mathrm{g})}(t) = \frac{e\phi_{\mathbf{k}_\perp}(0)}{T_i} F_{i0}\left[k_r^2 a_i^2 e^{-ik_r\overline{v}_{dr}t} - \mathcal{K}_L(t) \times \left(1 - \frac{1}{4}k_r^2\rho^2\right)\left(1 - e^{-ik_r\overline{v}_{dr}t}\right)\right] \quad \text{for } \kappa^2 < 1$$

(helically trapped)

$$\delta f_{i\mathbf{k}_\perp}^{(\mathrm{g})}(t) = \frac{e\phi_{\mathbf{k}_\perp}(0)}{T_i} F_{i0}\left[k_r^2 a_i^2 - \mathcal{K}_L(t)\left\{ik_r\left(\Delta_r - \langle\Delta_r\rangle_{\mathrm{po}}\right) + \frac{1}{2}k_r^2\left(\Delta_r - \langle\Delta_r\rangle_{\mathrm{po}}\right)^2\right\}\right] \quad \text{for } \kappa^2 > 1.$$

(helically untrapped)

These are derived from taking the average along the rapid particle motion along the field line.

Perturbed gyrocener distribution

$\delta f(v_\parallel, v_\perp)$

Helical plasma

$q=1.5,\ \varepsilon_h=0.1,\ L=2,\ M=10$
$t=12.5\ (R_0/v_{ti})$

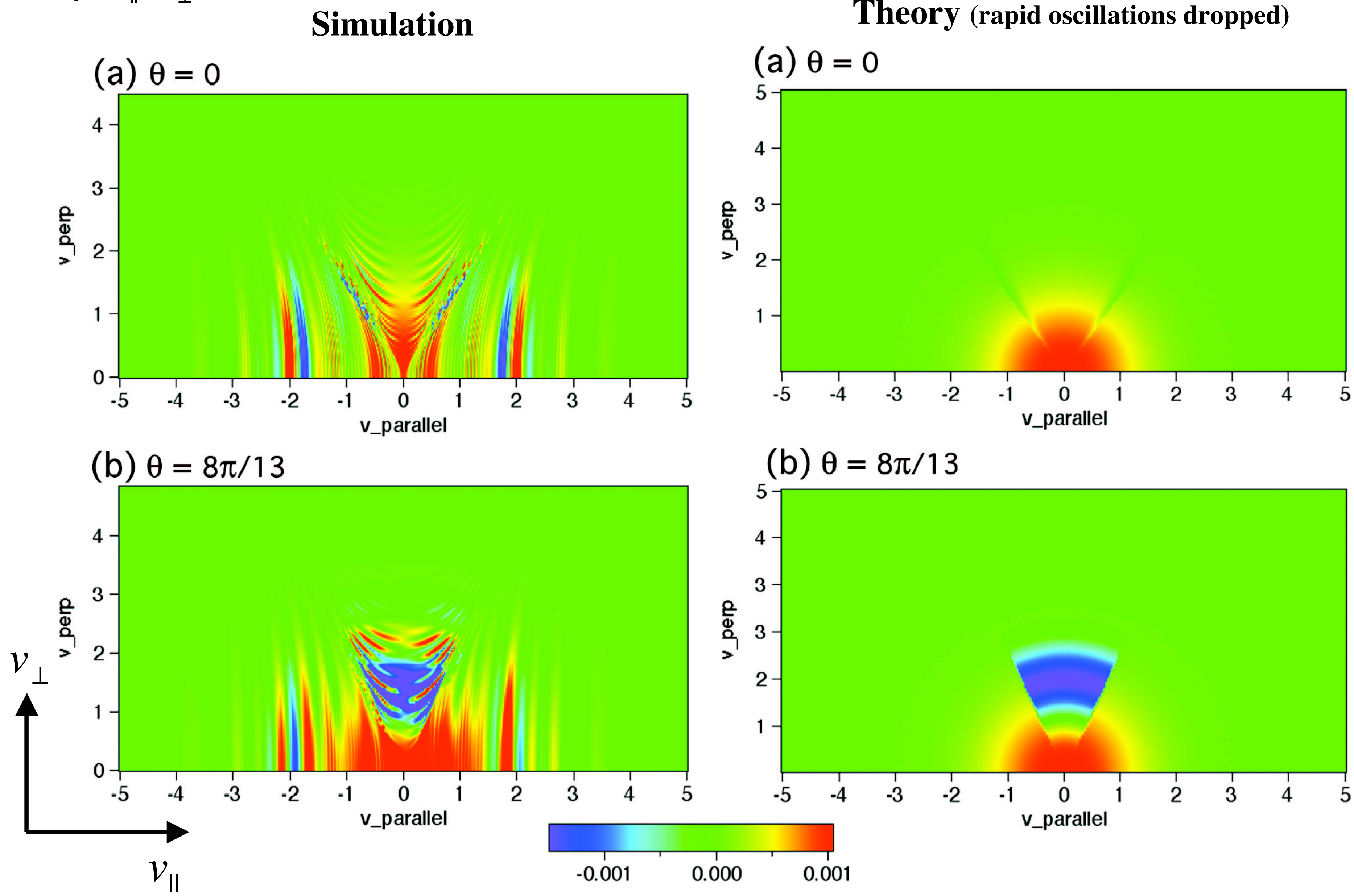

In the LHD experiments, better confinement is observed in the inward-shifted magnetic configurations, where lower neoclassical ripple transport but more unfavorable magnetic curvature driving pressure-gradient instabilities are anticipated.

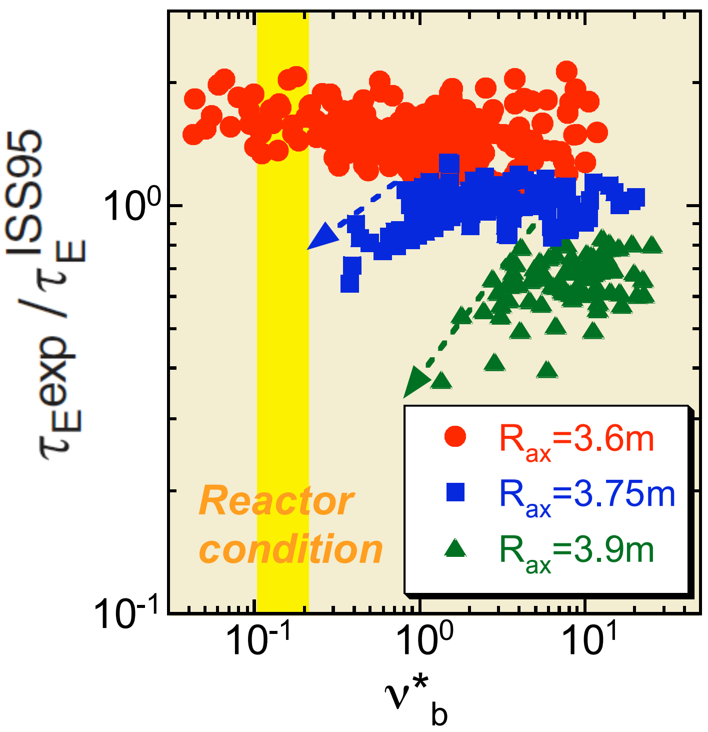

H. Yamada *et al.* (PPCF2001)

Anomalous transport is also improved in the inward shifted configuration.

In this work,

we investigate effects of changes in helical magnetic configuration on anomalous transport and zonal flows based on ITG turbulence simulation and zonal-flow response theory to show that neoclassical optimization contributes to reduction of anomalous transport by enhancing the zonal-flow level.

Standard and Inward-shifted configurations

Inward ➡ slightly more unstable

bad curvature

good curvature

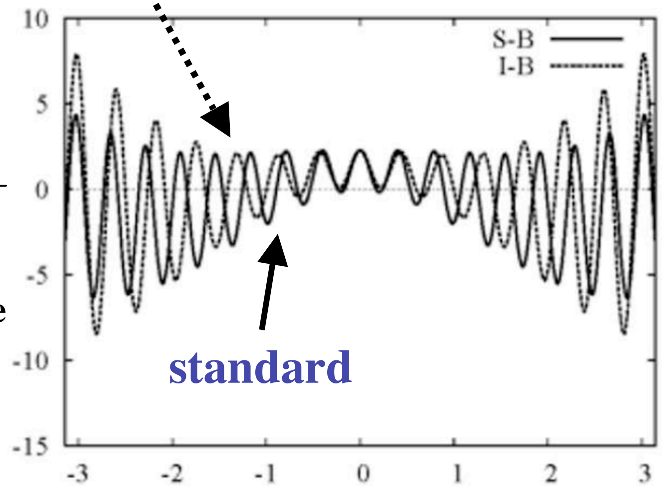

Magnetic curvature along the fieldline

|*B*| along the fieldline

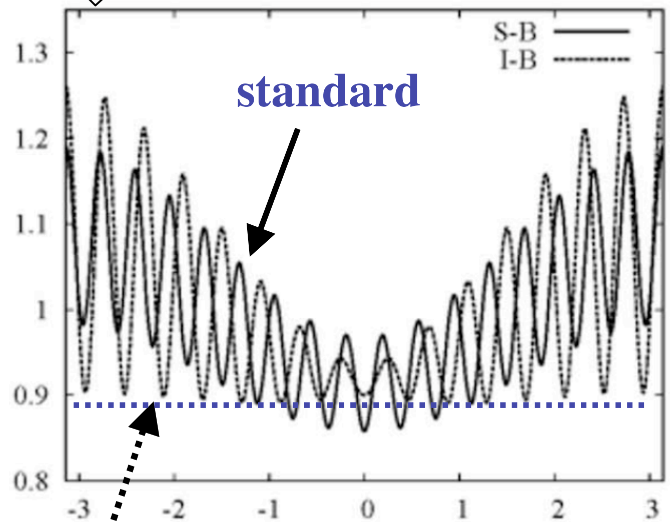

Inward

➡ smaller neoclassical transport

Magnetic surface at $r = 0.6\,a$

Safety factor

q = 1.9 (standard) 1.7 (inward)

Magnetic shear parameter

s = -0.85 (standard) -0.96 (inward)

r/R_0	ε_t	$\varepsilon_h/\varepsilon_t$	$\varepsilon_-/\varepsilon_t$	$\varepsilon_+/\varepsilon_t$
0.099	0.087	0.91	-0.28	0.0
0.114	0.082	1.20	-0.74	-0.24
$r\varepsilon_{00}'/\varepsilon_t$	$r\varepsilon_t'/\varepsilon_t$	$r\varepsilon_h'/\varepsilon_t$	$r\varepsilon_-'/\varepsilon_t$	$r\varepsilon_+'/\varepsilon_t$
0.22	1,02	1.96	-0.63	0,0
0.71	1.00	2.44	-0.36	-0,61

Growth rates γ and real frequencies ω_r of ITG modes

The maximum growth rate is slightly larger for the inward-shifted case.

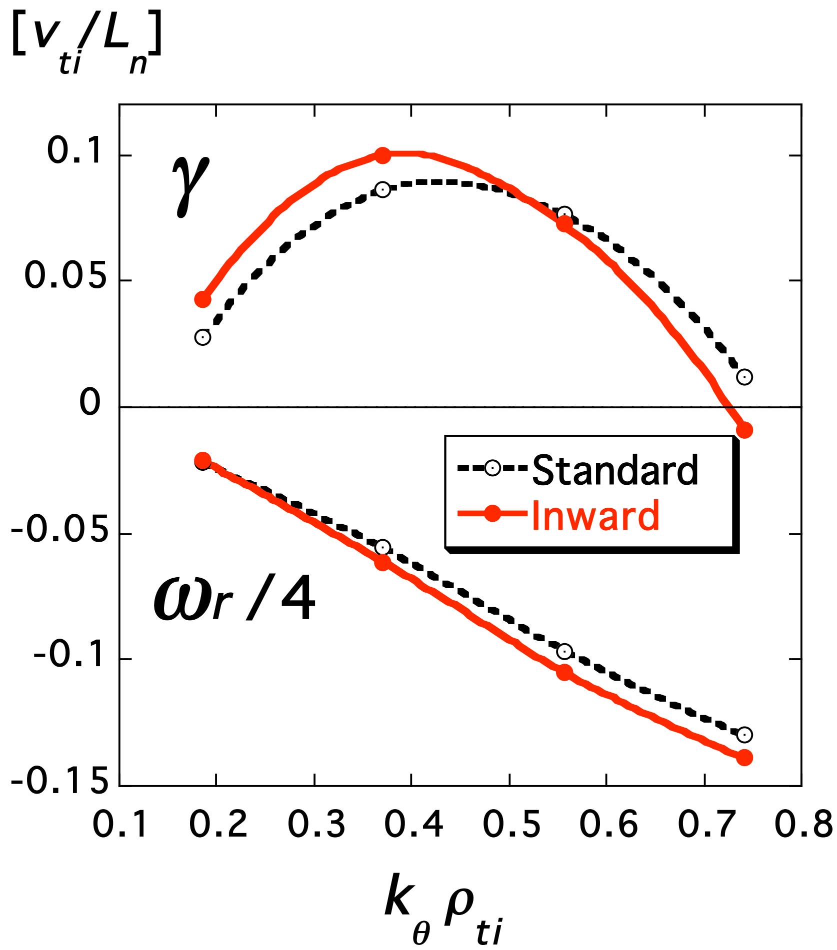

For the inward-shifted case, more unfavorable curvature but lower q and higher magnetic shear s.

$\eta_i = L_n/L_{Ti} = 3$

$L_n/R_0 = 0.3$

$T_e/T_i = 1$

Zonal-flow responses for the standard and inward-shifted configurattions

$k\,\rho_{ti} = 0.25$

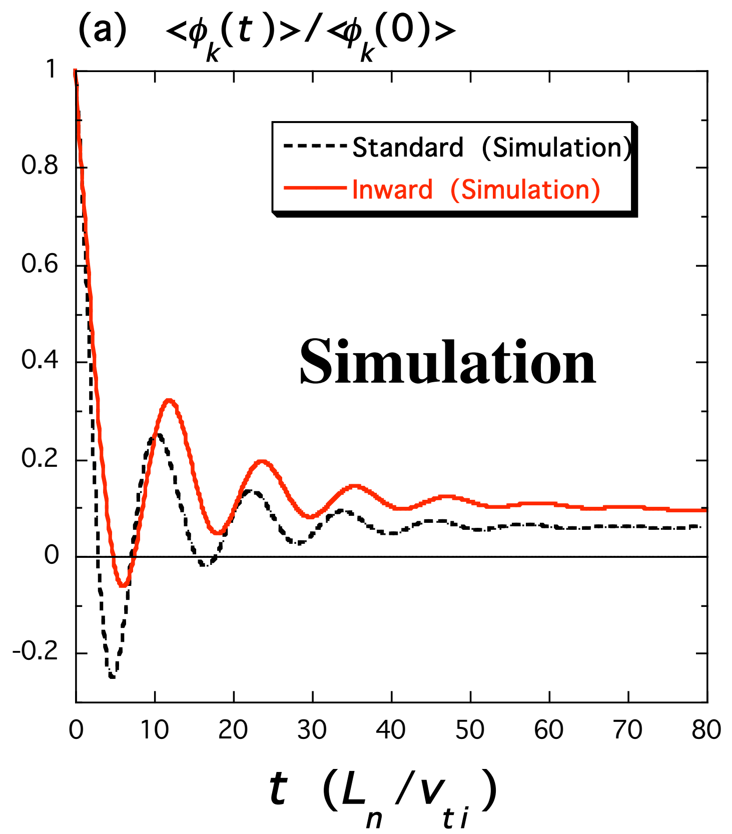

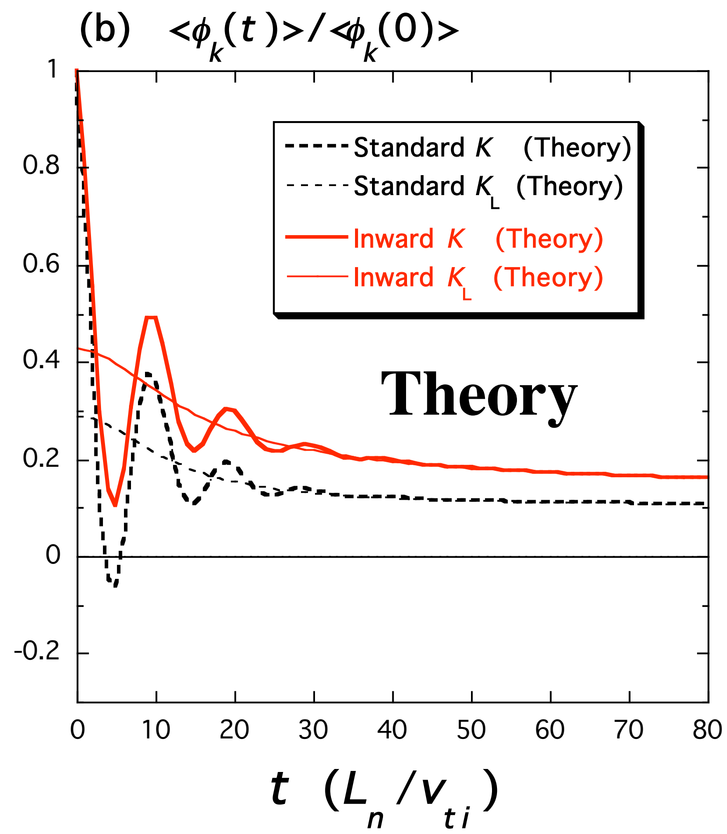

Theoretical predictions of GAM oscillation damping and residual zonal flow enhanced in the inward-shifted configuration are in qualitative agreement with simulation results.

Higher zonal-flow response for the inward-shifted configurattion is caused by slower radial drift of helical-ripple-trapped particles.

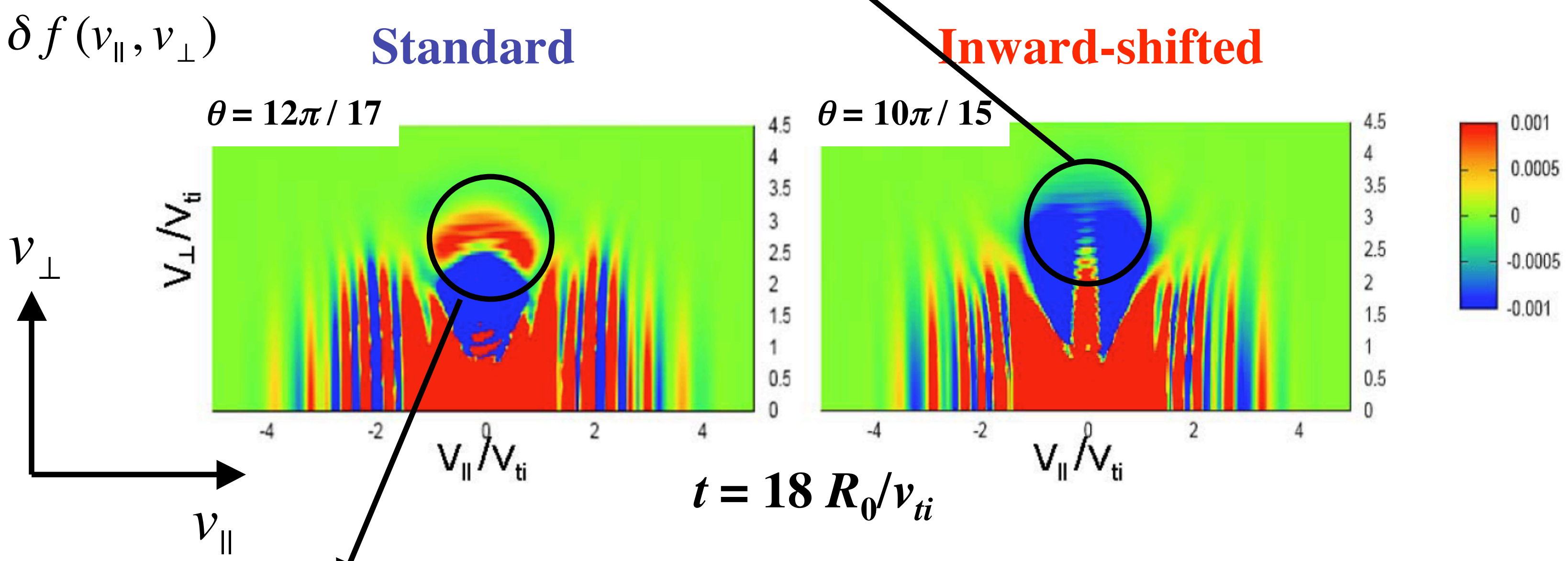

Oscillatory distribution produced by radial drift of helically-trapped particles gives higher shielding of potential and lower zonal-flow response.

Gyrokinetic Simulation of ITG Turbulence and Zonal Flows in LHD Plasma

Watanabe, Sugama, & Ferrando, PRL(2008)

Sugama Watanabe, & Ferrando, PFR(2008)

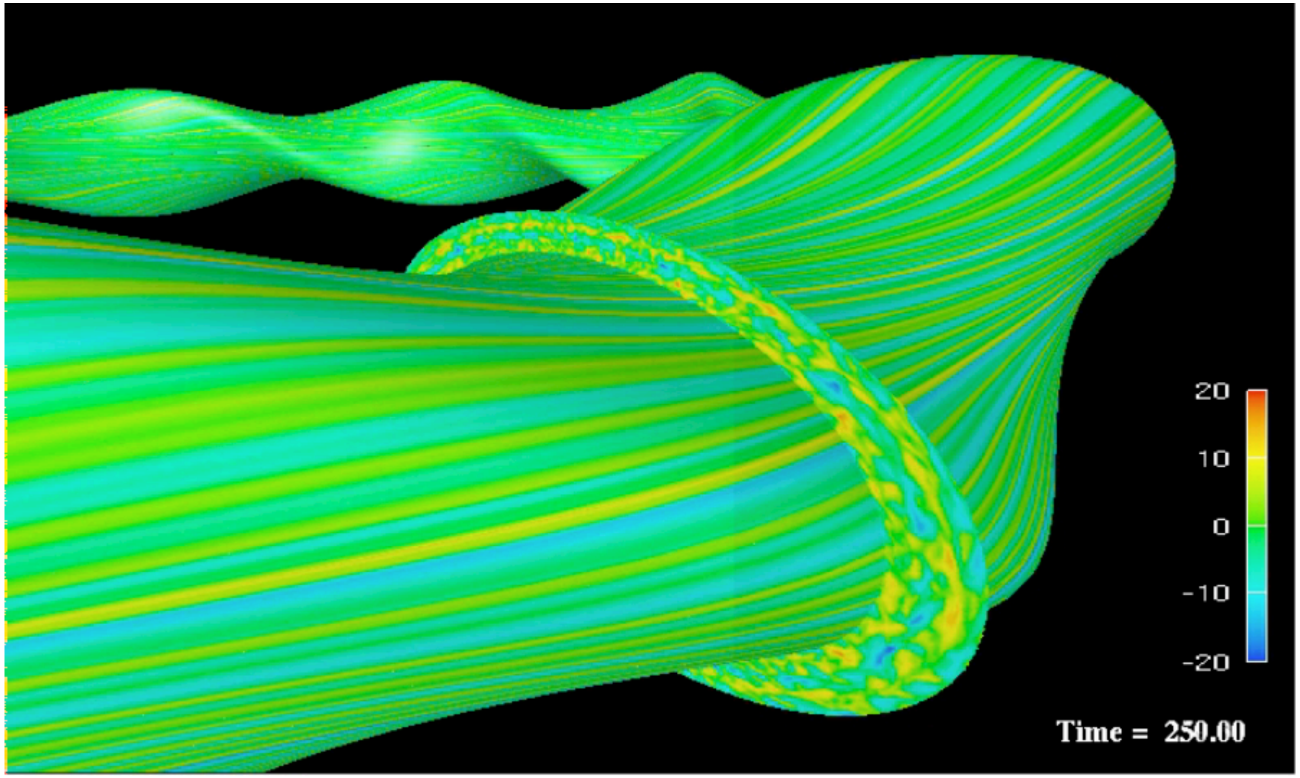

Color contours of electrostatic potential

More than 50 billions of grid points used in 5D phase space

$$N_x \cdot N_y \cdot N_z \cdot N_{v\parallel} \cdot N_{v\perp} = 128 \times 128 \times 512 \times 128 \times 48 \approx 5.15 \times 10^{10}$$

EARTH SIMULATOR

The gyrokinetic Vlasov simulations of the ITG turbulence were carried out by the Earth Simulator under the support from JAMSTEC.

ITG Turbulence Simulations for the Standard and Inward-Shifted Configurations in LHD

Smaller χ_i and larger zonal flows are found in the saturated turbulent state for the inward-shifted configuration than for the standard one !

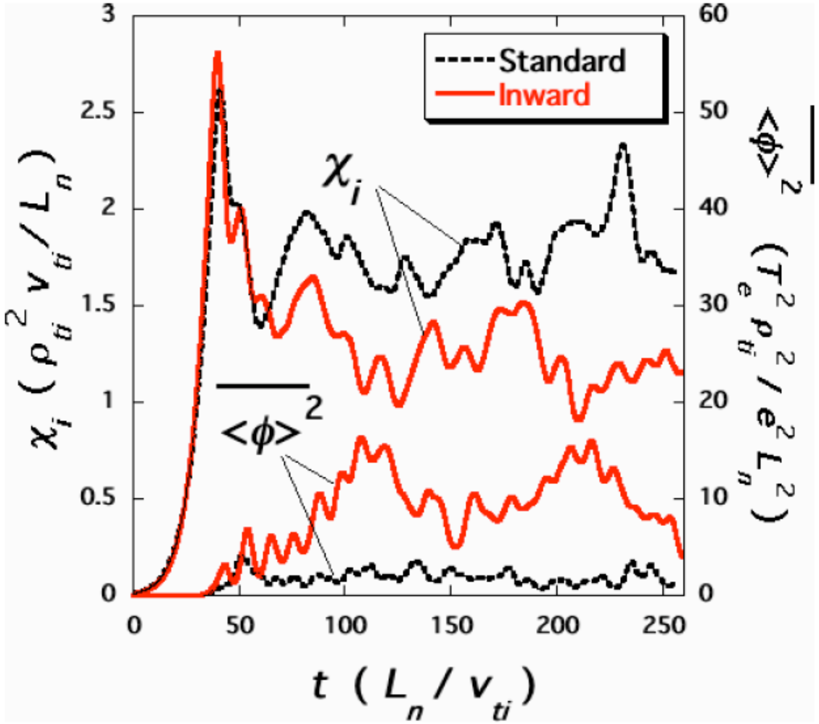

Turbulent thermal diffusivity and squared zonal-flow potential

$$\overline{\langle\phi\rangle^2} = \int_0^\infty S(k_r) dk_r$$

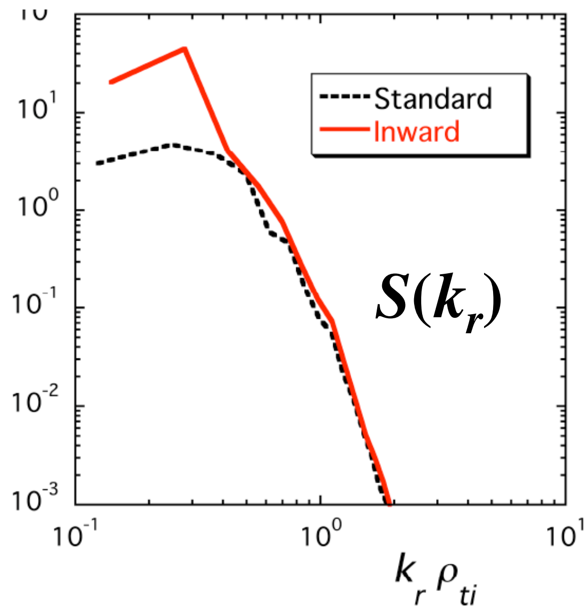

k_r spectrum of zonal-flow potential (averaged over $60 < t < 250$)

ITG Turbulence and Zonal Flows in LHD Plasma

Color contour of potential perturbations

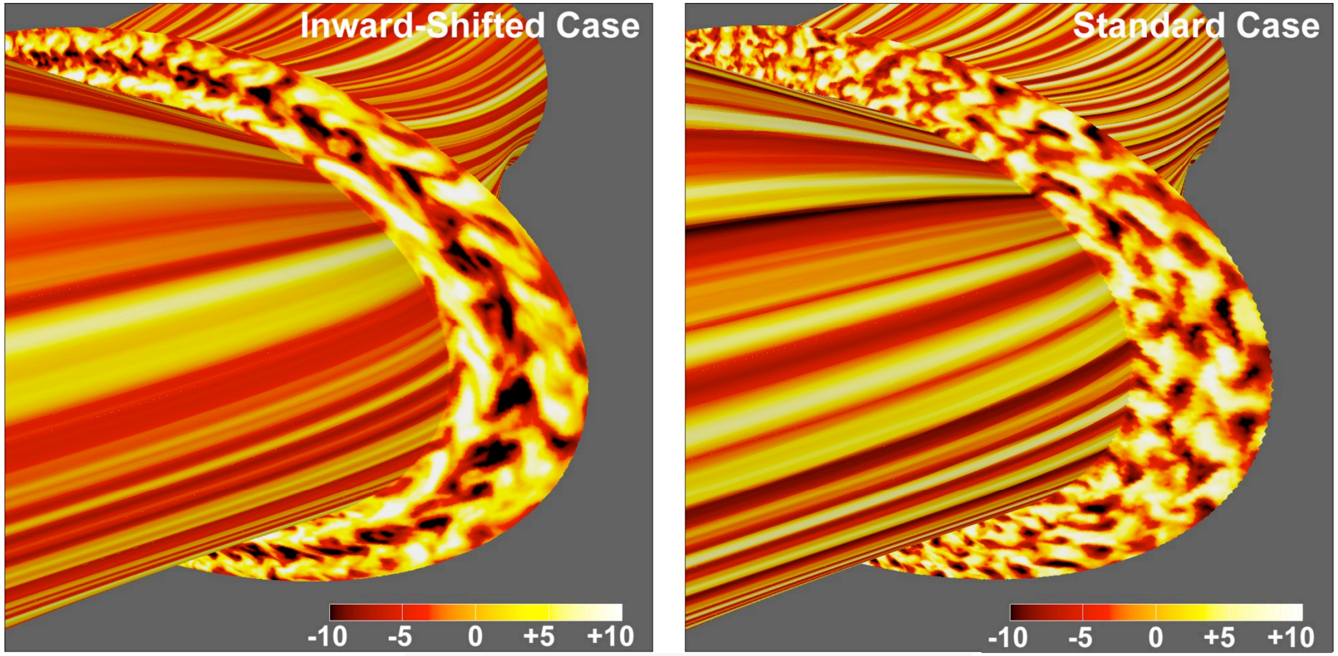

inward-shifted configuration

standard configuration

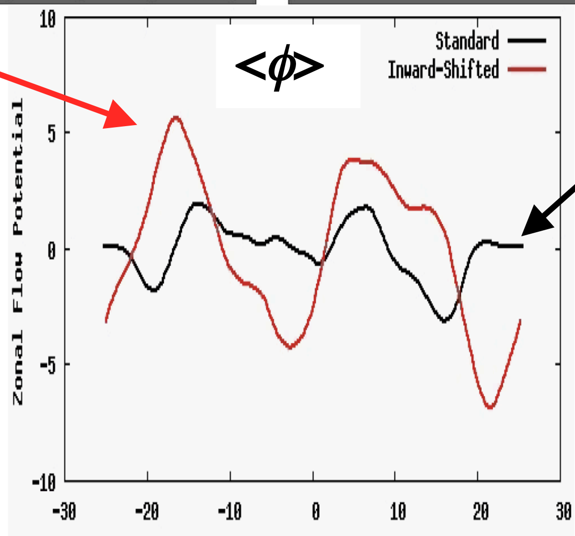

$(r-r_0)/\rho_{ti}$ ($r_0 = 0.6\,a$)

Radial profiles of zonal-flow potential $<\phi>$

$$\overline{\langle\phi\rangle^2} = \int_0^\infty S(k_r)dk_r$$

k_r spectrum of zonal-flow potential

$S(k_r)$

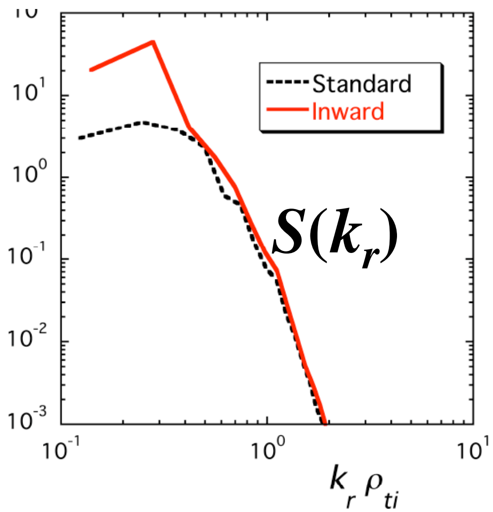

stationary part

$S_0(k_r)$

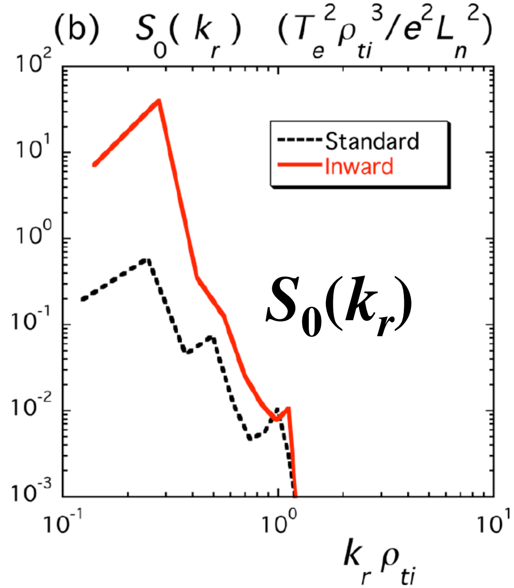

Profiles of zonal-flow potential

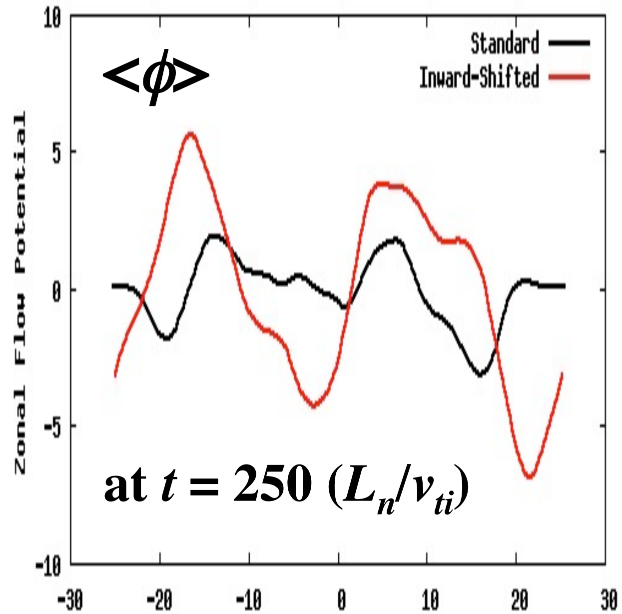

$(r\text{-}r_0)/\rho_{ti}$ (r_0 = 0.6 a)

Time-averaged $<\phi>$

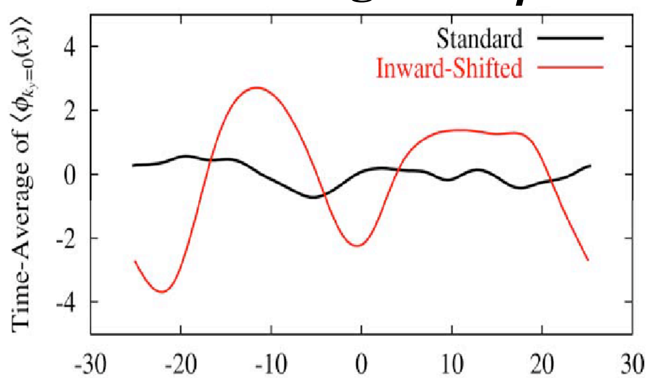

$(r\text{-}r_0)/\rho_{ti}$ (r_0 = 0.6 a)

Larger stationary zonal flows are generated in the inward-shifted configuration.

Spatio-Temporal Profiles of Zonal-Flow Potential

Inward-shifted configurations

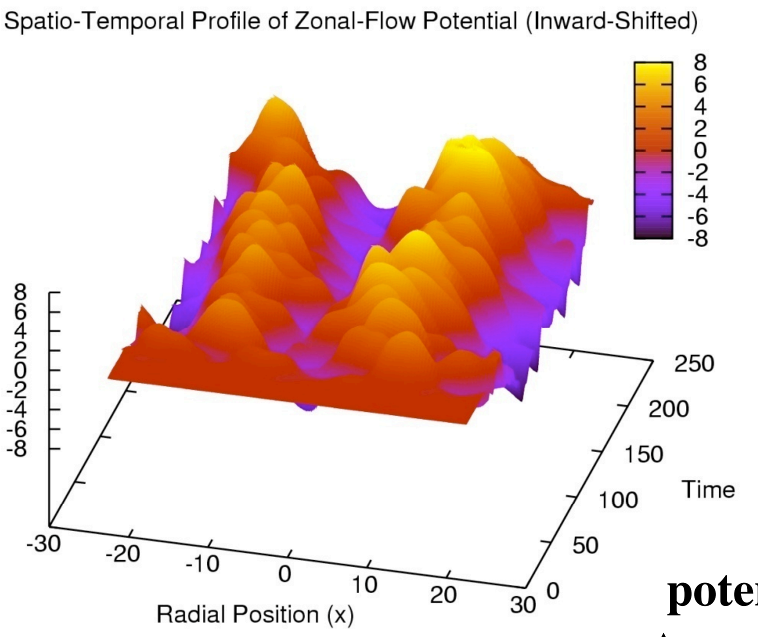

Standard configurations

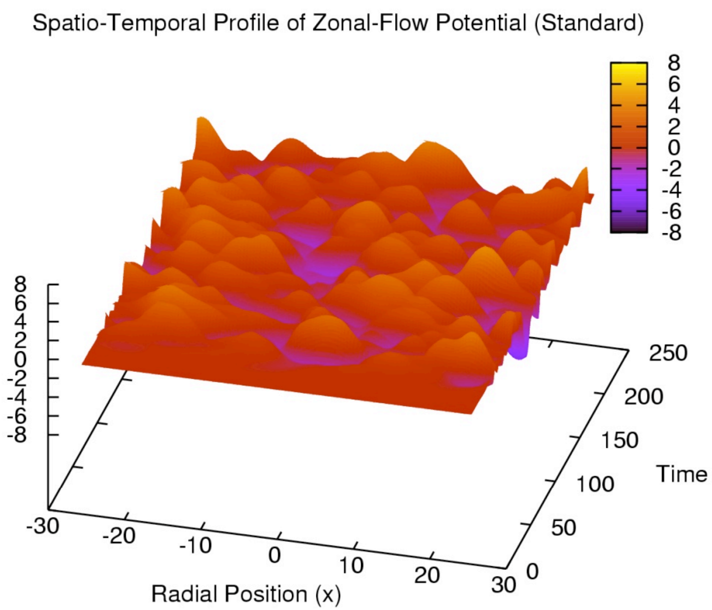

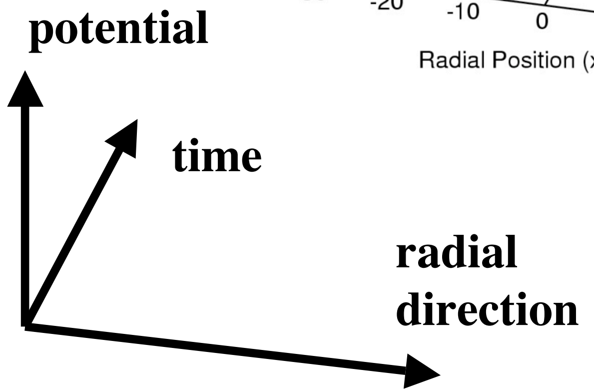

Summary

- Zonal flows are an attractive mechanism to regulate plasma turbulence and it is important to optimize geometry for enhancing residual zonal flows which reduce anomalous transport.
- A kinetic-fluid closure model to describe zonal flow dynamics (residual zonal flow and GAM damping) in tokamaks is presented.
- Effects of changes in helical magnetic configuration on anomalous transport and zonal flows are investigated based on ITG turbulence simulation and zonal-flow response theory.
- The inward-shifted LHD configuration enhances zonal-flow generation and reduces turbulent thermal diffusivity even though it is linearly more unstable.
- Thus, neoclassical optimization contributes to reduction of anomalous transport by increasing residual zonal flows.
  This gives a physical mechanism to explain better confinement observed in the LHD experiments with the inward plasma shift.